Neurological Disorders and Stroke International

Research Article
Published: 10 May, 2022

SHCBP1: A Novel Potential Molecular Target for Pan-Cancer Therapy

*Xiaorong Zhao[1], Wenzhuo Wang[1], Dandan Li[1], Qingjuan Li[1], Yuxuan Zhang[1] and Bo Niu[1,2]**

[1]Department of Biochemistry and Molecular Biology, Shanxi Medical University, China

[2]Department of Biotechnology, Beijing Municipal Key Laboratory of Child Development and Nutriomics, China

Abstract

Purpose: Although many experimentally validated evidence and clinical data support the link between SHCBP1 (SHC-Binding and Spindle-Associated 1) and cancer, there is no pan-cancer analysis available. Based on various databases, we analyzed the roles assumed by SHCBP1 in different cancers to provide new targets for cancer therapy.

Methods: We used versatile public databases such as TIMER, Interactive Analysis of Gene Expression Profile, 2nd Edition (GEPIA), UALCAN, The Cancer Genome Atlas (TCGA), cBioPortal, Clinical Bioinformatics Assistant, DiseaseMeth, TISIDB, Human Protein Atlas (HPA), STRING and Database for Annotation, Visualization, and Integrated Discovery (DAVID) to analyze SHCBP1 expression, mutation, methylation in tumors, as well as its survival analysis, tumor-immune interactions and functional networks.

Results: SHCBP1 was highly expressed in most tumors leading to poor prognosis and the degree of expression was positively correlated with the degree of infiltration by activated memory CD4+ T cells. We observed cancer-associated fibroblast infiltration in Breast Invasive Carcinoma (BRCA), Renal Clear Cell Carcinoma (KIRC) and Thyroid Cancer (THCA). Protein kinase activity and microtubules can influence gene enrichment, while "cell cycle", "oocyte meiosis" and "viral carcinogenesis" are possible pathways of SHCBP1 involvement in tumorigenesis.

Conclusion: Altogether, our first pan-cancer analysis of SHCBP1 demonstrated its potential as a biomarker for tumor prognosis diagnosis or as a molecular target for immunotherapy.

Keywords: SHCBP1; Pan-cancer; Prognosis; Molecular targeted therapy

OPEN ACCESS

Correspondence:
Bo Niu, Department of Biochemistry and Molecular Biology, Shanxi Medical University, Taiyuan 030001, Shanxi, China,
E-mail: niub2004@126.com

Received Date: *02 May 2022*
Accepted Date: *09 May 2022*
Published Date: *10 May 2022*

Citation:
Zhao X, Wang W, Li D, Li Q, Zhang Y, Niu B. SHCBP1: A Novel Potential Molecular Target for Pan-Cancer Therapy. Neurol Disord Stroke Int. 2022; 4(1): 1026.

Introduction

The complex mechanisms of tumorigenesis and the high frequency of occurrence threaten humans, so it is crucial to perform pan-cancer analysis of any gene to assess its molecular biological relevance in clinical prognosis and pathogenesis. Based on the publicly funded The Cancer Genome Atlas (TCGA) project and the existing the Gene Expression Omnibus (GEO) database [1-5], we were able to target functional genomics datasets from different tumors for pan-cancer analysis. SHCBP1 (SHC-Binding and Spindle-Related 1), also known as a protein-coding gene, is a member of the Src homolog and collagen homolog (Shc) family, as well as a downstream Shc component of a novel signaling pathway. SHCBP1 may not only be engaged in the cell proliferation process, but also functions in regulating cell growth and differentiation. Functional analyses of how SHCBP1 evades the host immune response and what role it assumes in fibroblast growth factor signaling in neural progenitor cells during early embryonic development have also been performed from different perspectives of physiology and clinicopathology [6-8].

Previously, SHCBP1 has been reported to be inextricably linked to gastric cancer [9,10], penile [11] and prostate cancers [12]. In addition, diseases associated with SHCBP1 include lung cancer, synovial sarcoma and glioma, involving the β-catenin signaling pathway, TGF-β1/Smad signaling pathway and NF-κB signaling pathway [13-15]. However, although based on current animal or cellular experiments as well as clinical data, there is currently no evidence for a broad cancer association between SHCBP1 and various tumor types. Our study is the first to perform a pan-cancer analysis of SHCBP1 using online platforms such as TCGA and the Genotype-Tissue Expression (GTEx). We also explored the role of SHCBP1 in different carcinogenesis or potential mechanisms in prognosis in the context of gene expression, genetic alterations, immune infiltration,

immunohistochemistry, survival status and cellular pathways.

Materials and Methods

Gene expression analysis

We entered SHCBP1 into the "Gene_DE" module of TIMER2 (Tumor Immune Estimate Resource, Version 2) Web (http://timer.comp-genomics.org/) [16] to observe SHCBP1 expression in different TCGA tumors or in specific tumors, as well as differential expression in normal tissues adjacent to cancer. For tumors in which normal tissue was completely infiltrated or highly restricted, such as Adrenocortical Carcinoma (ACC) and invasive Breast Cancer (BRCA), we administered the GEPIA2 (Interactive Analysis of Gene Expression Profile, 2nd Edition) (http://gepia2.cancer-pku.cn) database's "Expression Analysis -Box Plots" module [17]. By adjusting the settings P-value cutoff =0.01, |log2fc| (fold change) cutoff =1, and "Match TCGA normal and GTEx data", box plots of the expression differences between pathological and normal tissues of these tumors were derived. In addition, the expression of SHCBP1 in all TCGA tumors at different pathological stages (stages I, II, III, IV) was presented as a violin plot by using the "Pathological Stage Map" module of GEPIA2. And the expression data transformed by log2 [TPM (Transcripts per Million) +1] were applied to violin plots. Notably, the UALCAN portal (http://ualcan.path.uab.edu/analysis-prot.html) [18] is an interactive portal that facilitates protein expression analysis on the CPTAC Oncology (Clinical Proteomics Analysis Consortium) dataset. We summarized the expression levels of total proteins in breast cancer, Ovarian Cancer (OV), Colon Cancer, Renal Cell Carcinoma (RCC), Uterine Endometrial Cancer (UCEC) and Lung Adenocarcinoma (LUAD) and in normal tissues by entering "SHCBP1".

Genetic alteration and methylation analysis

We selected "TCGA Pan-Cancer Atlas study" in the "Quick select" module of the cBioPortal webpage (https://www.cbioportal.org/) [19] and input "SHCBP1" to view its genetic change characteristics. The frequency of alteration, mutation type and Copy Number Alteration (CNA) results for all TCGA tumors were displayed under the "Cancer Type Summary" page. We applied the "Comparison/Survival" module to explore data on whether SHCBP1 gene alterations affect TCGA tumor survival, and to further validate this question, we also obtained Kaplan-Meier plots and Log-rank Test P-values [20,21]. By accessing the online website of Clinical Bioinformatics Assistant (https://www.aclbi.com), we entered the gene "SHCBP1" in its "Pan-Cancer" module, selected all tumor samples, and changed different methods to obtain the array maps for mutation analysis. DiseaseMeth [22,23] is a repository that focuses on the analysis of cross-sectional datasets of disease and normal samples to provide complete gene methylation data. We accessed version 2.0 of DiseaseMeth (http://bio-bigdata.hrbmu.edu.cn/diseasemeth/), checked "Cancer" in the "Disease" type under the "Analyze" page, and entered "SHCBP1" in the "Gene Symbol" box with other parameters unchanged. Finally, we observed the performance of SHCBP1 in different tumor types in the "Methylation Profile".

Immune infiltration analysis

It is well known that the immune system operates and functions continuously in both tumor development and treatment. Cancer-associated fibroblasts, located in and as constitutive components of the tumor microenvironment, can modulate tumor-infiltrating immune cell function and may advance the cancer pathology [24-27]. The correlations between SHCBP1 and immune infiltrates were investigated via the Clinical Bioinformatics Assistant website, TIMER2 and TISIDB. Notably, the TISIDB database (http://cis.hku.hk/TISIDB/index.php [28] is an integrated repository portal for tumor-immune system interactions. First, we explored the relationship between SHCBP1 expression and immune infiltration in all TCGA tumors by selecting all tumor samples and entering "SHCBP1" in the "Pan-Cancer Analysis - Immune Correlation" module of the Clinical Bioinformatics Assistant website. Secondly, different algorithms such as TIMER, MCPCOUNTER, CIBERSORT, CIBERSORT-ABS, QUANTISEQ, XCELL and EPIC were provided in the "Immune-Gene" module of TIMER2 web server for us to evaluate the immune infiltration of SHCBP1 gene and in tumor-associated fibroblasts. P-values and partial correlation (cor) values were obtained by a purely corrected Spearman rank correlation test, and the data are visualized as heat and scatter plots. Finally, we logged into the TISIDB database, searched for the "SHCBP1" gene symbol and clicked on the "Immunomodulator" module to view separately the "Immunoinhibitor" and "Immunostimulator" to obtain heat maps of SHCBP1 expression and immunosuppressive and immunostimulatory agents across different human tumor types with respect to Spearman correlation. We also obtained correlations between a specific tumor and different immune agents, and the data are presented in the form of scatter plots. Major Histocompatibility Complex (MHC), a tightly interlocking group of genes located on the short arm of human chromosome 6, is also known as Human Leukocyte surface Antigens (HLA). The relationship between MHC and the immune system is mutually fulfilling and unsurprisingly figures in the pathogenesis and development of almost all complex diseases, including tumor [29-32]. During the immunization of the body, antibodies on the surface of T cells recognize antigens, provided that all antigens are processed and bound to the cell surface by MHC molecules. This is also true in cancer cells, and the mechanism is illustrated in Figure 1. Thus, we captured the association between SHCBP1 expression levels and MHC molecules in different tumors.

Immunohistochemistry

We logged into the Human Protein Atlas (HPA) [33,34] database (https://www.proteinatlas.org/) and searched for "SHCBP1". In the "RNA AND PROTEIN EXPRESSION SUMMARY" under the "TISSUE" section, we clicked on "Lung", "Female tissues" and "Male tissues", and obtained immunohistochemical images of normal lung, breast, and prostate tissues, respectively. In the "PATHOLOGY" section, "PROTEIN EXPRESSION" was used to obtain immunohistochemical images of LUAD, Lung Squamous Carcinoma (LUSC), breast cancer, and Prostate Carcinoma (PRAD), respectively.

Survival prognosis analysis

We entered the "SHCBP1" gene into the "Pan-cancer Analysis" module of the Clinical Bioinformatics Assistant website and performed prognostic analysis of 33 tumors in the TCGA database to obtain Overall Survival (OS), Progression Free Survival (PFS), Disease Free Survival (DFS) and Disease Specific Survival (DSS) forest plots. To collect OS and DFS data plots of SHCBP1 in all TCGA tumors, we turned on the "Survival Map" mode of GEPIA2. We set the expression threshold interval as Cutoff-high (50%) and Cutoff-low (50%) as the boundary to distinguish between high and low expression. Among them, the log-rank test was adopted and the final survival plot was available under "Survival Analysis".

SHCBP1-related gene enrichment analysis

Based on the protein resource integration tool, STRING (https://string-db.org/) [35], we put the protein name/identifier "SHCBP1" and the organism "*Homo sapiens*" to search the site. Next, we selected the main parameters: the minimum required interaction score ["Low confidence (0.150)"], the network edge meaning "evidence", the maximum number of interactors shown as "no more than 50 interactors" in 1st shell and the active interaction sources "experiments". Based on the above screening, a map of proteins bound to SHCBP1 was generated. The top 100 target genes associated with SHCBP1 were available for all TCGA tumor and normal tissue datasets under the "Similar Gene Detection" module of GEPIA2. "Correlation Analysis" module under paired Pearson correlation analysis made it clear whether SHCBP1 and established gene expression were associated. Log2 TPM was displayed while P-values and correlation coefficients (R) have also been indicated in the dot plot. In addition, we adopted the heat map data of the selected genes provided by the "Gene_Corr" module of TIMER2, which included Spearman's partial correlation (cor) and purity-adjusted P-value rank correlation tests. JVENN [36], an interactive VENN graphical viewer, was used by us to compare SHCBP1 binding and interacting genes. By combining two sets of data, we performed Kyoto Encyclopedia of Genes and Genomes (KEGG) pathway analysis of SHCBP1. This was done by uploading the gene list to DAVID (Database for Annotation, Visualization, and Integrated Discovery) (https://david.ncifcrf.gov/) [37] by selecting the identifier ("official") and species "*Homo sapiens*" settings as a way to collect data for functional annotation maps. Finally, the data were visualized as horizontal bar graphs and bubble plots using GraphPad Prism 9 software and the HIPLOT website (https://hiplot.com.cn/), respectively. In addition, we exported the Biological Process (BP), Cellular Component (CC) and Molecular Function (MF) data on the DAVID website and enriched them with Gene Ontology (GO) analysis, which was finally processed into two-dimensional bar graphs by Excel 2016 software.

Statistical analysis

In this paper, we applied the Wilcox test to compare gene expression differences. Pearson correlation analysis was used to determine the relationship of SHCBP1 with other similarly expressed genes. For survival analysis, we performed log-rank tests and calculated risk ratios (HR) based on the Cox proportional risk (PH) model. TIMER, CIBERSORT, CIBERSORT-ABS, QUANTISEQ, XCELL, MCPCOUNTER, and EPIC algorithms were applied for the estimation of immune infiltration. P-values and partial correlation (cor) values were obtained by Spearman's rank correlation test with purity adjustment. Survival analysis was performed using Kaplan-Meier analysis, log-rank test and Cox regression test. In addition, the statistical significance obtained from the calculations was annotated by the number of stars (*: p-value <0.05; ***: p-value <0.01; ***: p-value <0.001). Because of the extremely large sample size we designed, we chose a more conservative approach for each multiple comparison, namely the bonferroni correction, which was included in the R language's built-in method to adjust a range of p-values in an attempt to limit the probability of false discovery (type I error, incorrectly rejecting the null hypothesis when there was no real effect).

Results

Gene expression analysis data

After manipulating the TIMER2 database, we analyzed the expression of SHCBP1 in TCGA for each cancer type and concluded that it was higher in various tumors than in the corresponding normal tissues (Figure 2a). In Bladder Urothelial Carcinoma (BLCA), BRCA, Cholangiocarcinoma (CHOL), Colonic Adenocarcinoma (COAD), Esophageal Carcinoma (ESCA), Glioblastoma Multiforme (GBM), Head and Neck Squamous Cell Carcinoma (HNSC), Renal Chromophobe (KICH), Renal Papillary Cell Carcinoma (KIRP), Hepatocellular Carcinoma of the Liver (LIHC), LUAD, LUSC, PRAD, Rectal Adenocarcinoma (READ), Gastric Adenocarcinoma (STAD), Thyroid Cancer (THCA), and UCEC at P<0.001. SHCBP1 in Cervical Squamous Cell Carcinoma and Endocervical Adenocarcinoma (CESC), Pheochromocytoma and Paraganglioma (PCPG) (P<0.01) and renal clear cell carcinoma of the Kidney (KIRC), Cutaneous Melanoma (SKCM) (P<0.05) showed high expression in all of them.

We assessed the difference in SHCBP1 expression between tumor tissues of ACC, BRCA, Lymphoma Diffuse Large B-cell Lymphoma (DLBC), OV, Thymoma (THYM) and Uterine Sarcoma (UCS) and normal tissues after using normal tissues of the GTEx dataset as controls (Figure 2b, P<0.01). However, for pathological and normal tissues of Acute Myeloid Leukemia (LAML), Low-Grade Glioma of the brain (LGG), Sarcoma (SARC) or Testicular Germ Cell Tumor (TGCT), we failed to obtain significant differences between them. We also observed the correlation between SHCBP1 expression and pathological stages of cancers, including ACC, BLCA, KICH, KIRP, LIHC, LUAD, LUSC and TGCT, using the "Pathological Stage Map" module of GEPIA2 (Figure 2c, all P<0.05), while the correlation with other cancers was not significant. Total SHCBP1 protein expression was higher in BRCA than in normal tissues (P<0.001), rendered as a box plot by Figure 2d. There was no significant expression difference in OV compared to normal controls, whereas statistically significant differences were observed in UCEC and LUAD (P<0.01). In addition, protein expression of SHCBP1 was not shown in primary tissues of COAD and KIRC.

Genetic alteration and methylation analysis data

We investigated the genetic alterations of SHCBP1 occurring in TCGA tumors. From Figure 3a, we can see that patient with UCEC had the highest frequency of SHCBP1 alterations (>4%), with "mutation" being the predominant type and the smallest percentage of "amplification" type. In prostate cancer cases, deep deletion was the most predominant type, showing an alteration frequency of 2.5%.

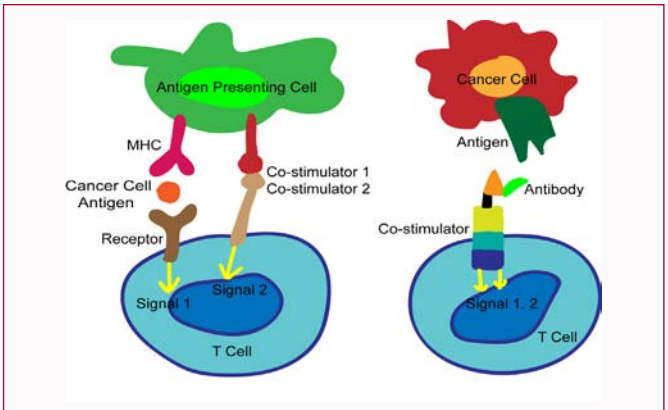

Figure 1: Cancer cell surface signals were presented to immune cells *via* MHC with co-stimulatory factors processing. The antigen-presenting cells first recognized the specific cancer antigen through MHC and delivered it to the surface receptors of the T cells, while the co-stimulatory factors acted to generate two signals in the T cells to stimulate them to perform immune functions.

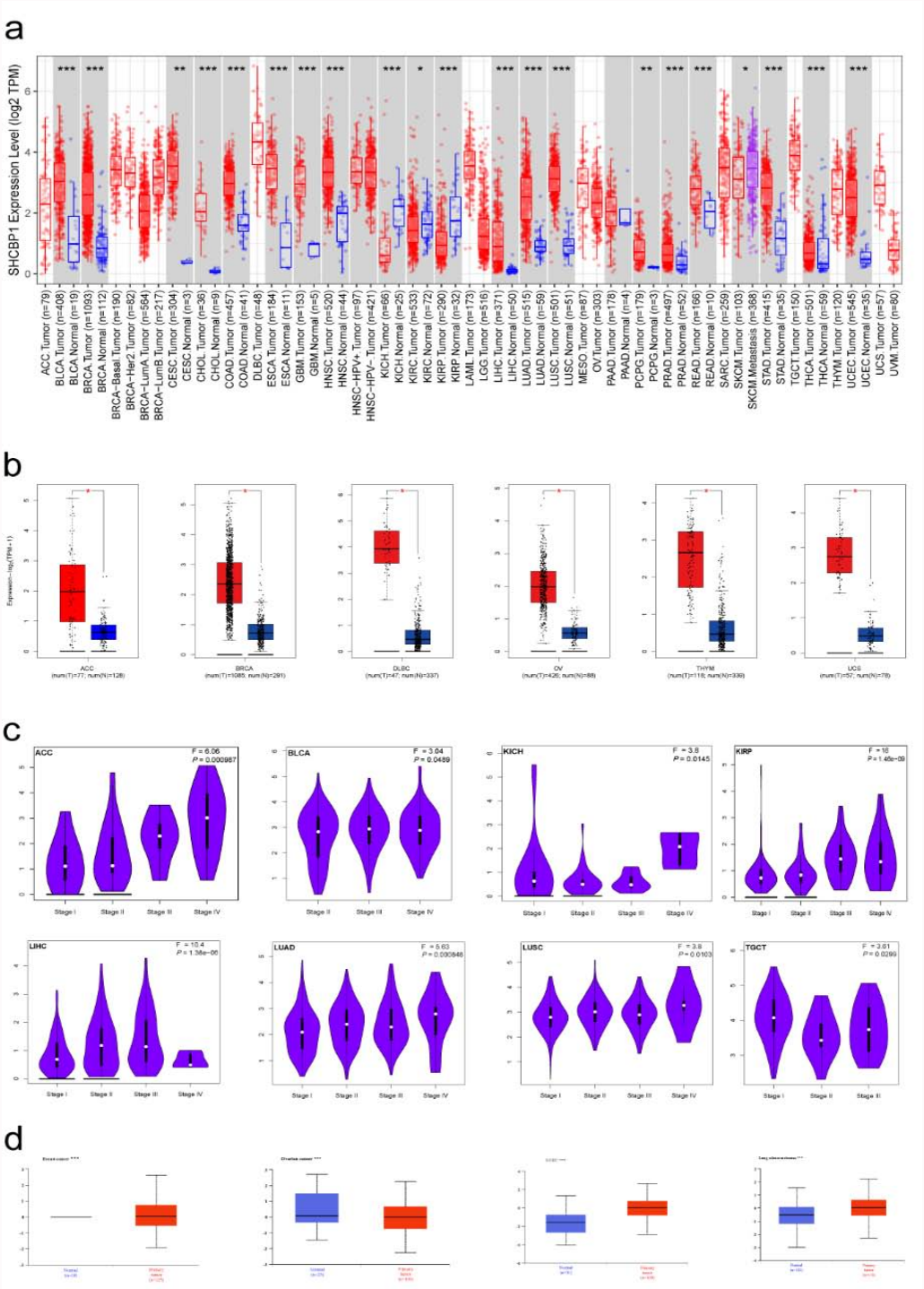

Figure 2: Analysis of SHCBP1 expression levels in different cancers. (a) Expression levels of SHCBP1 in cancer and paraneoplastic tissues in TCGA. (b) Expression levels of SHCBP1 in cancer and paraneoplastic tissues in TCGA and GTEx. (c) Correlation of SHCBP1 in different cancers with their pathological stages. (d) Total protein expression levels of SHCBP1 in BRCA, OV, LUAD, UCEC.

Notably, all DLBCs had copy number deletions of SHCBP1 with a frequency of about 2%. Apart from the above, it further described the type, site and number of cases of SHCBP1 gene alterations. The Clinical Bioinformatics Assistant website was again applied to determine the relationship between SHCBP1 expression in all tumors and Tumor Mutational Burden (TMB) as well as Microsatellite Instability (MSI), respectively. The results in Figure 3b illustrated that TMB negatively correlated with SHCBP1 expression in THYM, ESCA, TGCT, etc., while a positive correlation was found in STAD, BRCA, LGG, LUAD and PRAD. As for MSI, SHCBP1 expression was negatively correlated with it in DLBC, KICH, TGCT and Pancreatic Adenocarcinoma (PAAD). In contrast, there was a positive correlation between the two in STAD, UCEC and SARC (Figure 3c). Given that at most 1 transcript in each selected tumor type sample was aberrantly methylated, we were unable to develop a heat map of the results of SHCBP1 methylation in different tumors.

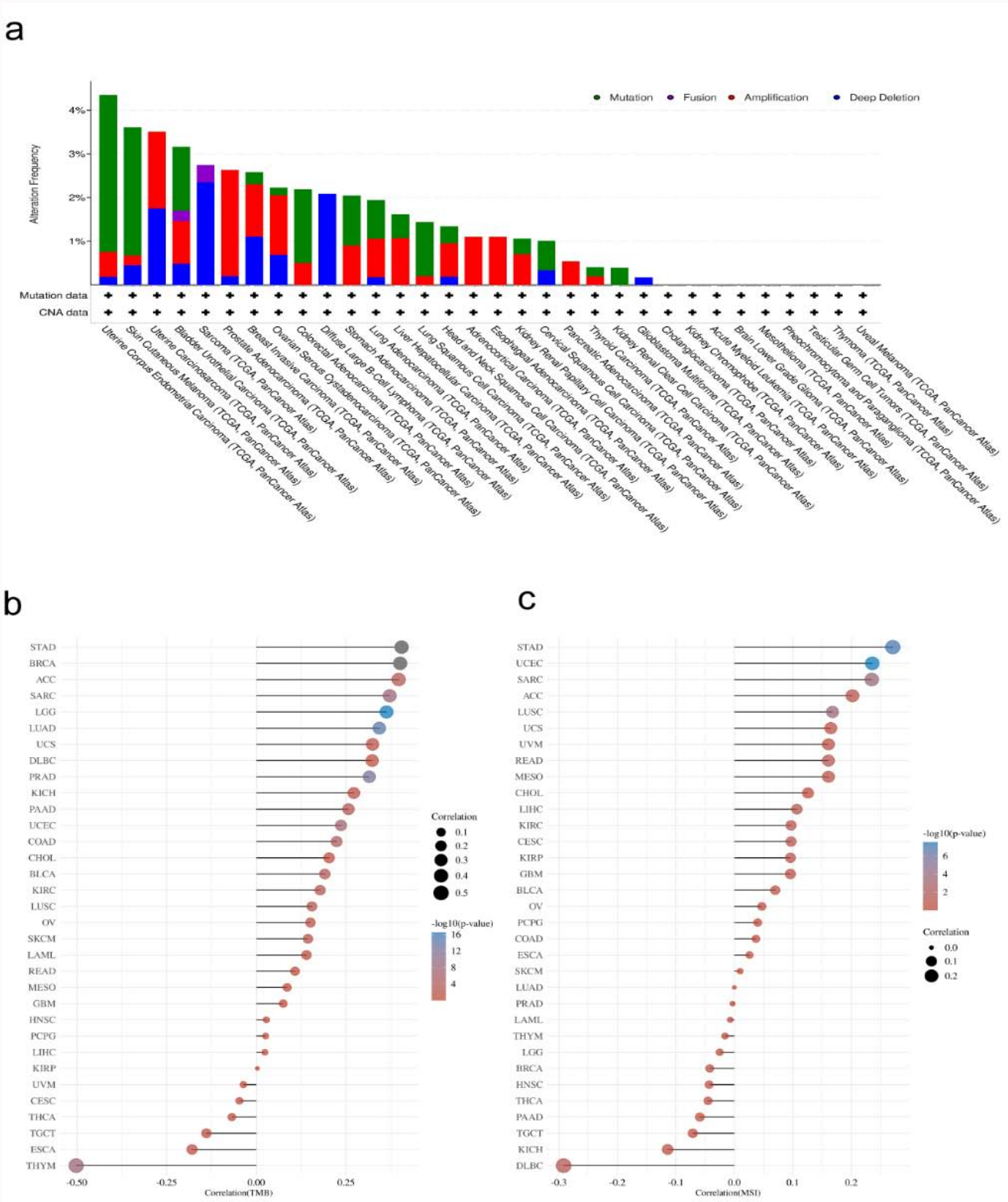

Figure 3: Alteration and methylation analysis of SHCBP1 in different cancers. (a) Mutation type, CNA of SHCBP1 in cancers. (b) TMB of SHCBP1. (c) MSI analysis of SHCBP1 mutations.

Immunity infiltration analysis data

We gained insight into the immunological knowledge of SHCBP1 by knowing its relevance to tumor immune infiltrating cells in an immunological context from Figure 4a. Here, after a series of analyses, we noted that SHCBP1 expression in BRCA, STAD and TGCT followed a statistically opposite trend to the estimated infiltration values of cancer-associated fibroblasts (P<0.05), while it also displayed the scatter plot data generated in the TIMER2 data base using this algorithm for the above-mentioned tumors (Figure 4b). For example, based on the XCELL algorithm, the expression level of

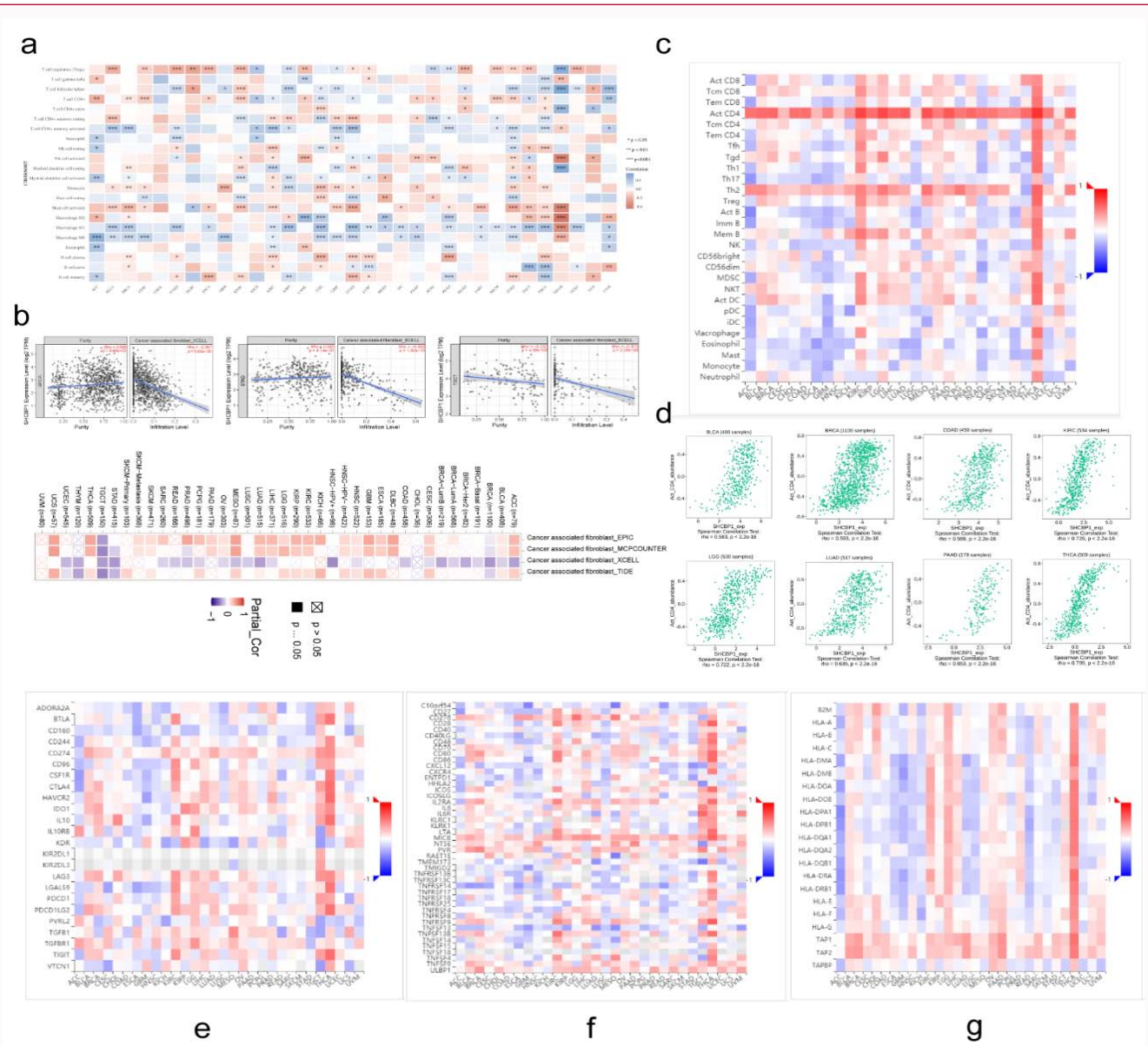

Figure 4: Immuno-infiltration analysis of SHCBP1. (a) Correlation between tumor infiltrating cells and SHCBP1. (b) Heat map of SHCBP1 correlation with cancer-associated fibroblasts and scatter plot in BRCA, STAD and TGCT (P<0.05). (c) Scatter plot of TIL abundance in relation to SHCBP1 expression. (d) Scatter plot of Act_CD4 abundance in relation to SHCBP1 correlation in specific tumors. Influence of different immunosuppressive (e) and immunostimulatory agents (f) on SHCBP1 gene expression levels in different tumors. (g) Heat map of the relationship between MHC molecules and SHCBP1.

SHCBP1 in BRCA and the degree of infiltration of cancer-associated fibroblasts were statistically significant (cor = -0.397, P=5.80e-39). In Figure 4c, we explored the relationship between the abundance of Tumor Infiltrating Lymphocytes (TIL) and SHCBP1 expression. With Gene Set Variation Analysis (GSVA), we can infer the relative abundance of TIL for each cancer type. The results in Figure 4c implied that SHCBP1 expression was statistically significantly and positively correlated with the infiltration abundance of Act_CD4 and Th2 cells in almost all tumor types. Moreover, the expression level of SHCBP1 in GBM and READ was negatively correlated with the abundance of TIL in the majority of tumors, while the opposite trend was observed in KIRC and THCA. In particular, the P-value of the correlation with Act_CD4 was less than 0.001 in tumors such as BLCA, BRCA, LGG, and so on (Figure 4d). As presented in Figures 4e-4f, they demonstrated the relationship between different immunosuppressive and immunostimulatory agents and the expression levels of SHCBP1 gene in different tumors, respectively. Among them, the gene expression in THCA exhibited a strong correlation with almost all, whether with immunosuppressants or immunostimulants. In almost all tumors regarding expression, SHCBP1 was trending in the same direction as TAP1 and TAP2 (Figure 4g). Moreover, three tumors, namely ACC, LGG and THCA, manifested significant correlations with almost all MHC molecules.

Immunohistochemical analysis data

We obtained typical immunohistochemical pictures of SHCBP1 in normal organisms and tumors from the HPA database. In Figure 5a, we enumerated the morphological pictures of normal lung, LUAD and LUSC at 200 μm under the microscope. Similarly, in Figure 5b, we presented the microscopic morphology of normal colon, normal

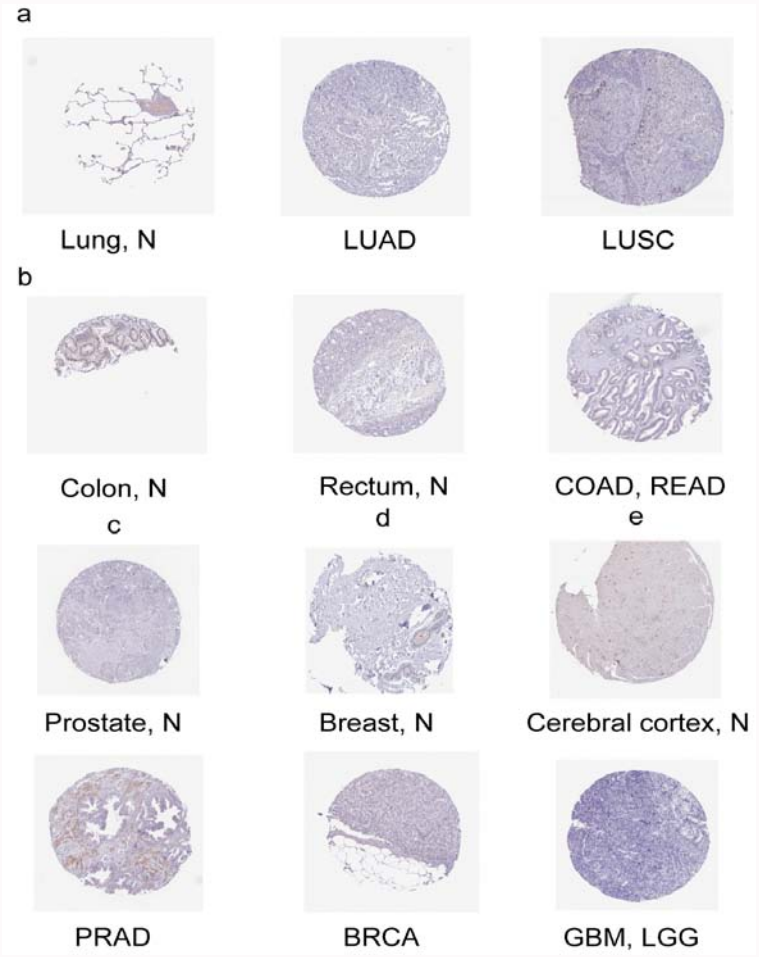

Figure 5: Immunohistochemical map of normal and cancerous tissues. Typical microscopic images of lung tissue, colorectal, prostate, breast, cortical normal tissues and their cancerous pathological tissues, where the antibodies were homogeneous in each group.

rectum and colorectal cancer, i.e., COAD and READ, in addition to the basic information about the patient such as gender, age, etc. While Figure 5c, 5d correspond to the male- and female-specific cancer types, PRAD and BRCA, respectively, their normal tissue morphology was also illustrated for comparison. To our knowledge, gliomas mostly infiltrated the cerebral cortex extensively, so we put immunohistochemical images of normal cerebral cortex and gliomas (GBM, LGG) in Figure 5.

Survival analysis data

We analyzed the survival data using the Clinical Bioinformatics Assistant website and presented the OS, DFS, PFS and DSS of SHCBP1 in different tumors in the form of a forest plot, where the length of the line segment corresponds to the 95% confidence interval and the size of the diamond square represents the weight, the shorter the line segment the more accurate the results (Figure 6a). Therefore, it can be seen that high expression of SHCBP1 correlates with OS in patients with ACC, KIRC, KIRP, LGG, LIHC, MESO, PAAD, PCPG, PRAD, READ, THYM, and UVM. In DSS, high SHCBP1 expression was correlated with KIRP, PAAD, PRAD. Meanwhile, after grouping cancer cases into high and low SHCBP1 expression levels, we then investigated whether there was any association between SHCBP1 expression derived from TCGA and GEO datasets and the prognosis of different patients, respectively. As shown in Figure 6b, in the TCGA project, high expression of SHCBP1 was correlated with ACC (P=3.7e-05), KIRP (P=0.0021), LGG (P=2.4e-08), LIHC (P=0.018), LUAD (P=0.00019), mesothelioma (MESO) (P=1.9e-07) and PAAD (P=0.028) in relation to OS. Data from DFS analysis (Figure 6c) showed that high expression of SHCBP1 was associated with ACC (P=0.0013), KICH (P=0.03), KIRP (P=0.00014), LGG (P=3.7e-07), LIHC (P=0.0058), LUAD (P=0.043), MESO (P=0.0014), PAAD (P=6e-04), PRAD (P=8e-04), and SARC (P=0.0024).

In addition, we applied the Kaplan-Meier mapper based on TCGA's Affymetrix chip information to further evaluate the survival associated with SHCBP1 (OS and RFS, as seen in Figure 6d, 6e, respectively). Interestingly, we found that SHCBP1 can be considered an unfavorable factor for the prognosis of BRCA, LIHC, PAAD, and SARC. SHCBP1 only affected RFS for BLCA (P=0.037), LUAD (P=0.03), OV (P=0.031), and UCEC (P=0.014), with no significant effect on their OS. Among them, for OV, high expression of SHCBP1 had a protective effect on RFS, of course, only for the holding database. For PCPG, SHCBP1 interfered with its OS in a statistically significant way (P=0.044), but not for RFS. Meanwhile, high levels of SHCBP1 expression showed protective effects on OS for READ (P=0.03) and STAD (P=0.023), but no significant effect on RFS. For ESCA, SHCBP1 had a protective effect on RFS (P=0.0083) but worsened its OS (P=0.02). In conclusion, altered expression levels of SHCBP1 implicated in the prognostic outcome of cancer patients.

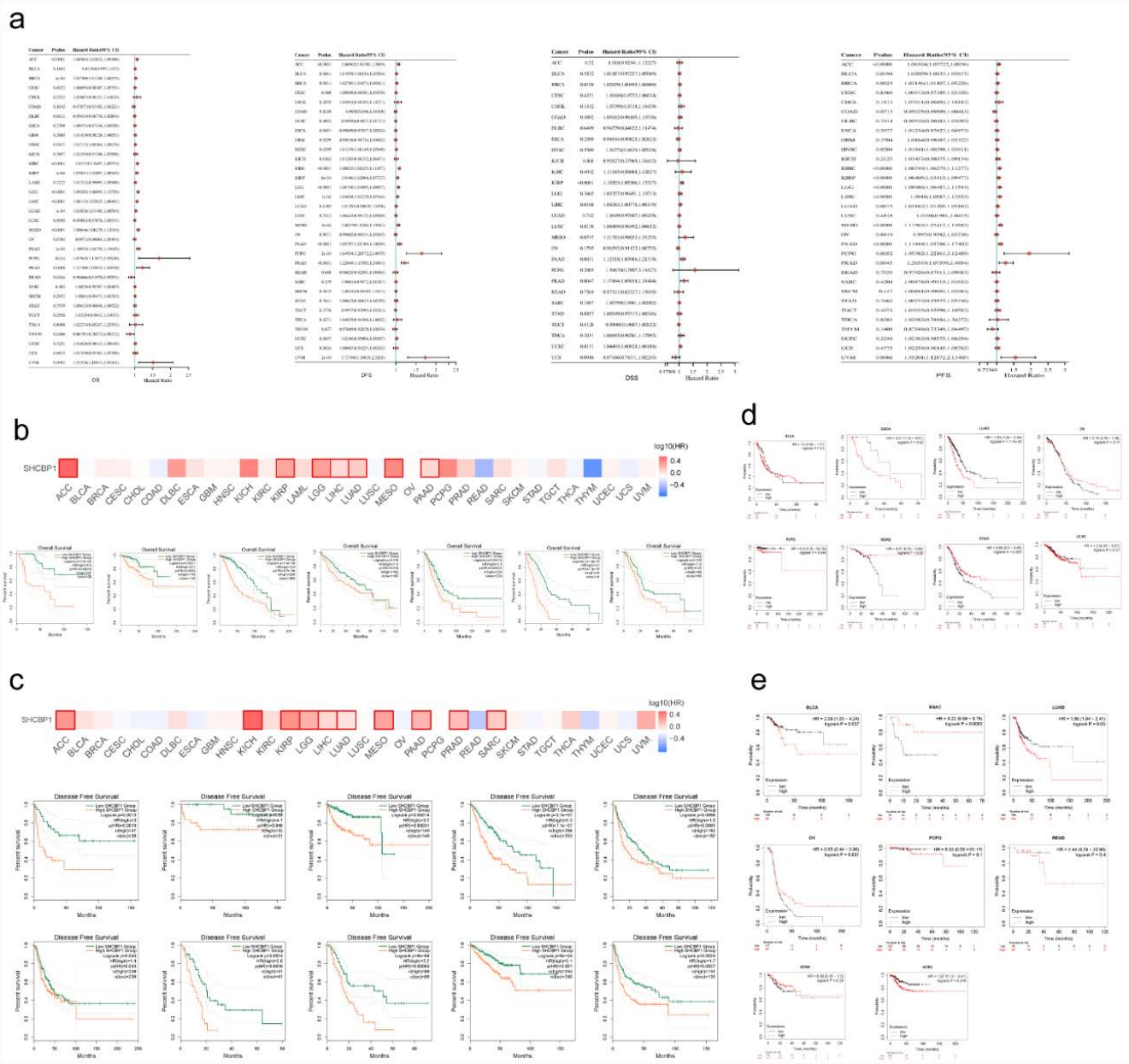

Figure 6: Analysis of SHCBP1 expression on the survival of tumor patients. Survival analysis of SHCBP1 expression on tumor patients. (a) Forest plot of the effect of SHCBP1 expression on OS, DFS, PFS, DSS in patients. Heat map of the effect of SHCBP1 expression levels on OS (b) and DFS (c) in tumor patients under TCGA database and survival curves in specific tumors. K-M plots of SHCBP1 expression on OS (d) and RFS (e) in tumor patients.

Enrichment analysis of SHCBP1-related partners

To sharpen the academic view of how the SHCBP1 gene affected tumorigenesis, we screened for pathways targeting SHCBP1 binding proteins and cross-tabulation of SHCBP1 expression-related genes. By searching the STRING tool, we gained 50 SHCBP1-binding proteins supported by experimental evidence. The network of these protein interactions is depicted in Figure 7a. In addition, we combined GEPIA2 and TCGA tumor expression data to identify the top 100 genes associated with SHCBP1 expression. Corresponding heat map data suggested that gene expression of targeting selection was positively correlated with SHCBP1 expression in cancers (Figure 7b). As displayed in the scatter plot in Figure 7c, SHCBP1 was positively correlated with the expression levels of many related genes, such as NCAPG (Non-SMC Condensin I complex, subunit G) (R=0.73), KIF23 (Kinesin Family member 23) (R=0.71), GTSE1 (G-2 and S-phase Expression 1) (R=0.70), and DLGAP5 (Disc, Large (Drosophila) Homology-Associated Protein 5) (R=0.69), GINS1 (Ginseng complex subunit 1) (R=0.58) and PRIM1 (primase, DNA, polypeptide 1) (R=0.57) (all P<0.001).

Based on these results, we took the intersection of these two analyses and found that they both covered five common members, namely CENPA, RACGAP1, KIF20A, KIF20B, and KIF23 (Figure 7d). We also combined these two datasets for KEGG and GO analysis of SHCBP1 functions. We presented the GO-enriched data in a bar chart in Figure 7e. MF data in GO analysis highlighted that most of these genes were associated with protein kinase activity or microtubules, such as microtubule binding, protein serine/threonine kinase activity, protein kinase activity, microtubule motor activity, etc. (Figure 7f). Microtubules, kinetochore, condensed chromosome kinetochore might be the main cellular components of genes, as seen in Figure 7g.

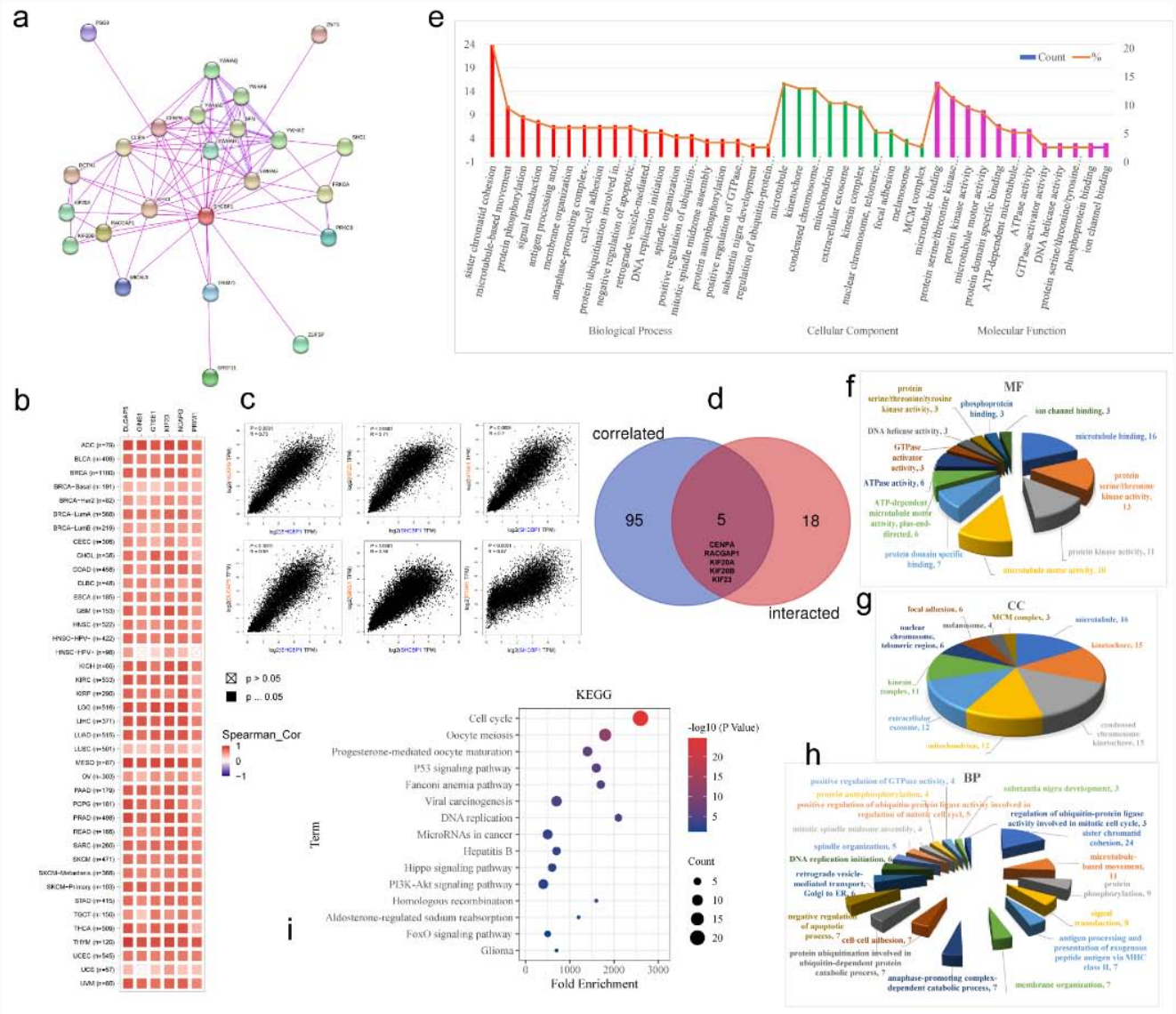

Figure 7: Gene and protein interaction network and enrichment analysis of SHCBP1. Gene and protein interaction network and enrichment analysis of SHCBP1. (a) Network mapping of experimentally validated proteins binding to SHCBP1. (b) Heat map data corresponding to genes with strong correlation with SHCBP1 in cancer. (c) Expression correlation analysis between SHCBP1 and selected target genes. (d) Cross-tabulation analysis profiles of SHCBP1 binding genes and related genes. (e) Histogram of GO analysis in general. Specific MF (f), CC (g), BP (h) pie charts of SHCBP1 in GO analysis. (i) Bubble plot of KEGG analysis of SHCBP1.

Also, we could speculate from the BP visualization diagram (Figure 7h): Genes were mainly linked to sister chromatid cohesion, microtubule-based movement, protein phosphorylation, signal transduction, antigen processing and presentation of exogenous peptide antigen *via* MHC class II, cell-cell adhesion, negative regulation of apoptotic process and other biological processes. The data in Figure 7i revealed that "cell cycle", "oocyte meiosis" and "viral carcinogenesis" may be pathways involved in tumorigenesis by SHCBP1.

Discussion

Pan-cancer analysis of genes or genomes potentially involved in cancer development based on public database platforms is of great relevance in many aspects of basic research, clinical practice, and theory derivation [38,39]. These studies can help us to understand which molecules are broadly involved in the development of human diseases and the processes or pathways they cover. In the current field of cancer research, many such molecules have been found to be differentially expressed or manifested across human cancers or a specific subtype, and given the complexity of cancer etiology and the uncertainty in our knowledge of this, it is essential to uncover more definitive genes that become factors in deepening our understanding of cancer. To this end, we have analyzed the expression of SHCBP1 in cancer and the role it may assume in this process.

Pan-cancer analysis can reveal tumor similarities and differences and provide insights into the design of cancer prevention and therapeutic targets [40]. Therefore, we examined the molecular characteristics of SHCBP1 expression, alterations, and DNA methylation in 33 tumors according to TCGA, CPTAC, and GEO databases. The outcome of SHCBP1 mostly highly expressed in tumors cannot be generalized either; after all, different tumors had different prognosis. Whether SHCBP1 in different tumors depended on a common molecular mechanism to induce disease development remained to be urgently investigated. Given that there is no relevant

literature on pan-cancer analysis of SHCBP1 from a holistic tumor perspective, we herein performed its differential expression and relationship with disease prognosis, TMB and MSI to elucidate the role of SHCBP1 in different cancers just to fill this gap.

In this study, we combined independent datasets from TCGA and GTEx to familiarize with SHCBP1 expression including in cancerous and normal tissues. The findings of SHCBP1 analysis in the 33 cancer datasets of TCGA implied that in BLCA [41], BRCA [42], CHOL, COAD, ESCA [43], GBM [44], HNSC, LIHC [45], LUAD [46], LUSC, PRAD, READ, STAD [10], THCA [47], and UCEC were expressed in large amounts, whereas they were less expressed in KICH, KIRC, and KIRP compared to normal tissues. Interestingly, we observed differences in gene expression in the two databases. And such differences in the same gene in different databases may be due to the influence of data collection methods and the mechanisms behind different biological features; hence SHCBP1 is not an exception. Buckley et al. [48] demonstrated that loss of SHCBP1 during T-cell development is directly affected by the regulation of CD4(+) T-cell effector function *in vivo*, rather than T-cell development, which is consistent with our results from immunological analysis of SHCBP1. Although many works have elucidated that high expression of SHCBP1 in certain cancers was accompanied by a negative prognosis, there has never been a study that provided an overview of the survival impact of this gene expression on patients with all types of cancers, and because of this our pan-cancer analysis can fill this gap and add to the foundation of SHCBP1 in cancer diagnosis and treatment. The cytoskeleton played an important role in the migration of normal and cancer cells, and microtubules were one of the components, as our GO analysis results showed that microtubule motility was one of the main biological processes of SHCBP1, and microtubules as its main cellular component while its molecular function was mainly expressed as microtubule binding. A recent study reported and described that microtubules and the upregulation of some factors regulating microtubule function compared to normal tissue, such as microtubule-associated proteins, end-tracking proteins or motor proteins, favored the highly aggressive nature of gliomas [49].

An increasing number of studies and reports have identified SHCBP1 as a cancer gene involved in the development and progression of many cancers. Thus, our study adds insight to the practice of SHCBP1 as a diagnostic marker in pan-cancer and for future advancement of its specific mechanistic studies. Recent researches have reported the involvement of SHCBP1 in the development of papillary thyroid carcinoma through targeting integrin and collagen formation and cellular stem cell pathways [47]. SHCBP1 was significantly upregulated in tumor tissues and its mRNA levels were negatively correlated with tumor-free survival of patients, and further analysis of the findings derived an increase in concomitant lymph node metastasis in patients with high SHCBP1 expression. Shi et al. [10] found that SHCBP1 released from the cascade axis is involved in regulating cell mitosis through biological processes such as translocation to the nucleus after Ser273 phosphorylation, while clinical evidence indicated that increased SHCBP1 predicted a poor clinical outcome of trastuzumab treatment in patients with gastric cancer. Ren et al. [43] discovered an upregulation of SHCBP1 expression in human esophageal squamous carcinoma tissue and confirmed this phenomenon correlated with the clinical characteristics of patients with esophageal squamous carcinoma. In contrast, in prostate cancer, Xu et al. [12] revealed that the overexpression of SHCBP1 benefited the cancer process, while patients with higher expression had poorer survival rates. In addition to this, SHCBP1 expression at high levels in synovial sarcoma [50] was downwardly associated with our analysis of the effect of SHCBP1 on patient survival, but not all cancer types exhibited high expression of SHCBP1. Gao et al. [51] discovered in their study of Long noncoding RNAs (lncRNAs) that SHCBP1 served as a tumor promoter and was lowly expressed in non-small cell lung cancer. The results of the work of Huang et al. [52] inferred that inhibition of SHCBP1 to achieve lower levels of inflammatory factors may be part of the mechanism why lignocaine A can be used against skin cancer. Our work laid the cornerstone for further identifying SHCBP1 as a therapeutic target and biomarker in its capacity as a tumor-promoting factor.

Overall, our pan-cancer study analyzed SHCBP1 differential expression in cancer, gene mutation and methylation, infiltration analysis in an immunological context, clinicopathological histochemistry, survival analysis and functional enrichment analysis based on multiple databases, and these data mapped a comprehensive landscape of SHCBP1 features in pan-cancer tumor types. Our results indicated that the SHCBP1 gene could be used as a potential prognostic biomarker for clinical diagnosis and evaluation of tumors.

References

1. Weinstein J, Collisson E, Mills G, Shaw K, Ozenberger B, Ellrott K, et al. The cancer genome atlas pan-cancer analysis project. Nat Genet. 2013;45(10):1113-20.
2. Tomczak K, Czerwińska P, Wiznerowicz M. The Cancer Genome Atlas (TCGA): An immeasurable source of knowledge. Contem Oncol (Pozn). 2015;19:A68-77.
3. Clough E, Barrett T. The gene expression omnibus database. Methods in Molecular Biology. 2016;1418:93-110.
4. Blum A, Wang P, Zenklusen JC. SnapShot: TCGA-analyzed tumors. Cell. 2018;173(2):530.
5. Liu J, Lichtenberg T, Hoadley K, Poisson L, Lazar A, Cherniack A, et al. An integrated TCGA pan-cancer clinical data resource to drive high-quality survival outcome analytics. Cell. 2018;173(2):P400-16.E11.
6. Chen J, Lai F, Niswander L. The ubiquitin ligase mLin41 temporally promotes neural progenitor cell maintenance through FGF signaling. Genes Dev. 2012;26(8):803-15.
7. Asano E, Hasegawa H, Hyodo T, Ito S, Maeda M, Takahashi M, et al. The Aurora-B-mediated phosphorylation of SHCBP1 regulates cytokinetic furrow ingression. J Cell Sci. 2013;126:3263-70.
8. Ito M, Iwasaki M, Takeda M, Nakamura T, Yanagi Y, Ohno S. Measles virus nonstructural C protein modulates viral RNA polymerase activity by interacting with host protein SHCBP1. J Virol. 2013;87(17):9633-42.
9. Dong Y, Yuan Y, Yu H, Tian G, Li D. SHCBP1 is a novel target and exhibits tumor-promoting effects in gastric cancer. Oncol Rep. 2019;41(3):1649-57.
10. Shi W, Zhang G, Ma Z, Li L, Liu M, Qin L, et al. Hyper activation of HER2-SHCBP1-PLK1 axis promotes tumor cell mitosis and impairs trastuzumab sensitivity to gastric cancer. Nat Commun. 2021;12(1):2812.
11. Mo M, Tong S, Yin H, Jin Z, Zu X, Hu X. SHCBP1 regulates STAT3/c-Myc signaling activation to promote tumor progression in penile cancer. Am J Cancer Res. 2020;10(10):3138-56.
12. Xu N, Wu Y, Yin H, Chen S, Li X, Xue X, et al. SHCBP1 promotes tumor cell proliferation, migration, and invasion, and is associated with poor prostate cancer prognosis. J Cancer Res Clin Oncol. 2020;146(8):1953-69.
13. Peng C, Zhao H, Song Y, Chen W, Wang X, Liu X, et al. SHCBP1 promotes synovial sarcoma cell metastasis via targeting TGF-β1/Smad signaling pathway and is associated with poor prognosis. J Exp Clin Cancer Res. 2017;36(1):141.

14. Zhou Y, Tan Z, Chen K, Wu W, Zhu J, Wu G, et al. Overexpression of SHCBP1 promotes migration and invasion in gliomas by activating the NF-κB signaling pathway. Mol Carcinog. 2018;57(9):1181-90.

15. Liu L, Yang Y, Liu S, Tao T, Cai J, Wu J, et al. EGF-induced nuclear localization of SHCBP1 activates β-catenin signaling and promotes cancer progression. Oncogene. 2019;38(5):747-64.

16. Li T, Fu J, Zeng Z, Cohen D, Li J, Chen Q, et al. TIMER2.0 for analysis of tumor-infiltrating immune cells. Nucleic Acids Res. 2020;48(W1):W509-14.

17. Tang Z, Kang B, Li C, Chen T, Zhang Z. GEPIA2: An enhanced web server for large-scale expression profiling and interactive analysis. Nucleic Acids Res. 2019;47:W556-60.

18. Chandrashekar D, Bashel B, Balasubramanya S, Creighton C, Ponce-Rodriguez I, Chakravarthi B, et al. UALCAN: A portal for facilitating tumor subgroup gene expression and survival analyses. Neoplasia. 2017;19(8):649-58.

19. Cerami E, Gao J, Dogrusoz U, Gross B, Sumer S, Aksoy B, et al. The cBio cancer genomics portal: An open platform for exploring multidimensional cancer genomics data. Cancer Discov. 2012;2(5):401-4.

20. Lundin J, Lundin M, Isola J, Joensuu H. Evaluation of a web-based system for survival estimation in breast cancer. Stud Health Technol Inform. 2003;95:788-93.

21. Győrffy B, Lanczky A, Eklund A, Denkert C, Budczies J, Li Q, et al. An online survival analysis tool to rapidly assess the effect of 22,277 genes on breast cancer prognosis using microarray data of 1,809 patients. Breast Cancer Res Treat. 2010;123(3):725-31.

22. Lv J, Liu H, Su J, Wu X, Liu H, Li B, et al. DiseaseMeth: A human disease methylation database. Nucleic Acids Res. 2012;40:D1030-5.

23. Xiong Y, Wei Y, Gu Y, Zhang S, Lyu J, Zhang B, et al. DiseaseMeth version 2.0: A major expansion and update of the human disease methylation database. Nucleic Acids Res. 2017;45:D888-95.

24. Bremnes R, Al-Shibli K, Donnem T, Sirera R, Al-Saad S, Andersen S, et al. The role of tumor-infiltrating immune cells and chronic inflammation at the tumor site on cancer development, progression, and prognosis: emphasis on non-small cell lung cancer. J Thorac Oncol. 2011;6(4):824-33.

25. Li B, Severson E, Pignon J, Zhao H, Li T, Novak J, et al. Comprehensive analyses of tumor immunity: Implications for cancer immunotherapy. Genome Biol. 2016;17(1):174.

26. Chen X, Song E. Turning foes to friends: Targeting cancer-associated fibroblasts. Nat Rev Drug Discov. 2019;18(2):99-115.

27. Nurmik M, Ullmann P, Rodriguez F, Haan S, Letellier E. In search of definitions: Cancer-associated fibroblasts and their markers. Int J Cancer. 2020;146(4):895-905.

28. Ru B, Wong C, Tong Y, Zhong J, Zhong S, Wu W, et al. TISIDB: An integrated repository portal for tumor-immune system interactions. Bioinformatics. 2019;35(20):4200-2.

29. Garcia-Lora A, Algarra I, Garrido F. MHC class I antigens, immune surveillance, and tumor immune escape. J Cell Physiol. 2003;195(3):346-55.

30. de Almeida D, Holoshitz J. MHC molecules in health and disease: At the cusp of a paradigm shift. Self Nonself. 2011;2(1):43-8.

31. Trowsdale J. The MHC, disease and selection. Immunol Lett. 2011;137(1-2):1-8.

32. Jiang J, Natarajan K, Margulies D. MHC Molecules, T cell receptors, natural killer cell receptors, and viral immunoevasins-key elements of adaptive and innate immunity. Adv Exp Med Biol. 2019;1172:21-62.

33. Pontén F, Schwenk J, Asplund A, Edqvist P. The human protein atlas as a proteomic resource for biomarker discovery. J Intern Med. 2011;270(5):428-46.

34. Thul PJ, Lindskog C. The human protein atlas: A spatial map of the human proteome. Protein Sci. 2018;27(1):233-44.

35. Szklarczyk D, Gable A, Nastou K, Lyon D, Kirsch R, Pyysalo S, et al. The STRING database in 2021: Customizable protein-protein networks, and functional characterization of user-uploaded gene/measurement sets. Nucleic Acids Res. 2021;49:D605-12.

36. Bardou P, Mariette J, Escudie F, Djemiel C, Klopp C. Jvenn: An interactive Venn diagram viewer. BMC Bioinformatics. 2014;15:293.

37. Dennis G, Sherman B, Hosack D, Yang J, Gao W, Lane H, et al. DAVID: Database for annotation, visualization, and integrated discovery. Genome Biol. 2003;4(5):P3.

38. Huntsman D, Ladanyi M. The molecular pathology of cancer: from pan-genomics to post-genomics. J Pathol. 2018;244(5):509-11.

39. Srivastava S, Hanash S. Pan-cancer early detection: Hype or Hope? Cancer Cell. 2020;38(1):23-4.

40. Schaub F, Dhankani V, Berger A, Trivedi M, Richardson A, Shaw R, et al. Pan-cancer alterations of the MYC oncogene and its proximal network across the cancer genome atlas. Cell Syst. 2018;6(3):P282-300.

41. Laukhtina E, Mori K, Mostafaei H, Merseburger A, Nyirady P, Moschini M, et al. Adverse events of the second-line treatment for patients with locally advanced or metastatic urothelial carcinoma of the bladder: Network meta-analysis. Immunotherapy. 2021;13(11).

42. Colak D, Nofal A, Albakheet A, Nirmal M, Jeprel H, Eldali A, et al. Age-specific gene expression signatures for breast tumors and cross-species conserved potential cancer progression markers in young women. PLoS One. 2013;8(5):e63204.

43. Ren C, Zhou Z, Wang X, Hua X, Zou M, Zhang X. SHCBP1 promotes the progression of esophageal squamous cell carcinoma via the TGFβ pathway. Appl Immunohistochem Mol Morphol. 2021;29(2):136-43.

44. Xuan C, Jin M, Wang L, Xue S, An Q, Sun Q, et al. PART1 and hsa-miR-429-mediated SHCBP1 expression is an independent predictor of poor prognosis in glioma patients. Biomed Res Int. 2020:1767056.

45. Long J, Bai Y, Yang X, Lin J, Yang X, Wang D, et al. Construction and comprehensive analysis of a ceRNA network to reveal potential prognostic biomarkers for hepatocellular carcinoma. Cancer Cell Int. 2019;19:90.

46. Zou A, Wu A, Luo M, Zhou C, Lu Y, Yu X. SHCBP1 promotes cisplatin induced apoptosis resistance, migration and invasion through activating Wnt pathway. Life Sci. 2019;235:116798.

47. Geng H, Guo M, Xu W, Zang X, Wu T, Teng F, et al. SHCBP1 promotes papillary thyroid carcinoma carcinogenesis and progression through promoting formation of integrin and collagen and maintaining cell stemness. Front Endocrinol. 2020;11:613879.

48. Buckley M, Arandjelovic S, Trampont PC, Kim TS, Braciale TJ, Ravichandran KS. Unexpected phenotype of mice lacking Shcbp1, a protein induced during T cell proliferation. PLoS One. 2014;9(8):e105576.

49. Otani Y, Ichikawa T, Kurozumi K, Date I. Dynamic reorganization of microtubule and glioma invasion. Acta Med Okayama. 2019;73(4):285-97.

50. Peng C, Zhao H, Chen W, Song Y, Wang X, Li J, et al. Identification of SHCBP1 as a novel downstream target gene of SS18-SSX1 and its functional analysis in progression of synovial sarcoma. Oncotarget. 2016;7(41):66822-34.

51. Gao W, Qi C, Feng M, Yang P, Liu L, Sun SH. SOX2-induced upregulation of lncRNA LINC01561 promotes non-small-cell lung carcinoma progression by sponging miR-760 to modulate SHCBP1 expression.J Cell Physiol. 2020;235(10):6684-96.

52. Huang H, Cai H, Zhang L, Hua Z, Shi J, Y Wei. Oroxylin A inhibits carcinogen-induced skin tumorigenesis through inhibition of inflammation by regulating SHCBP1 in mice. Int Immunopharmacol. 2020;80:106123.